Adsorption of arsenic by natural aquifer material in the San Antonio-El Triunfo mining area, Baja California, Mexico

A. Carrillo · J. I. Drever

Abstract Several experiments of arsenic (As) adsorption by aquifer material of the San Antonio-El Triunfo (SA-ET) mining area were conducted to test the feasibility of this material acting as a natural control for As concentrations in groundwater. This aquifer material is mineralogically complex, composed of quartz, feldspar, calcite, chlorite, illite, and magnetite/hematite. The total iron content (Fe_2O_3) in the fine fraction is ~12%, whereas Fe_2O_3 in the coarse fraction is <10 wt%. The experimental percent total As adsorbed vs. pH curves obtained match the topology of total As adsorbed onto iron oxi-hydroxides surface (arsenate + arsenite; high adsorption at low pH, low adsorption at high pH). A maximum of about 80% adsorbed in the experiments suggests the presence of arsenite in the experimental solutions. The experimental adsorption isotherm at pH 7 indicates saturation of surface sites at high solute concentrations. Surface titration of the aquifer material indicates a point of zero charge (PZC) for the adsorbent of about 8 to 8.5 (PZC for iron oxyhydroxides =7.9–8.2). Comparison between experimental and modeled results (using the MICROQL and MINTEQA2 geochemical modeling and speciation computer programs) suggests that As is being adsorbed mostly by oxyhydroxides surfaces in the natural environment. Based on an estimated retardation factor (R), the travel time of the As plume from the SA-ET area to La Paz and Los Planes is about 700 to 5000 years.

Key words Arsenic adsorption · Arsenic contamination · Oxyhydroxides surfaces

A. Carillo* (✉) · J. I. Drever
Dept. of Geology and Geophysics, University of Wyoming, Laramie, Wyoming 87201-3006, USA
*Current address: Depto. de Geologia UABCS, AP 19-B, La Paz, B.C.S., Mexico 23080
e-mail: carrillo@calafia.uabcs.mx

Introduction

Arsenic (As) is known for its toxicity to animals and humans (Fowle 1992; Enterline and others 1987; Goldman and Dacre 1991). Arsenic is also extensively recycled in the surface and near-surface environment (Bowell 1994a, 1994b; Ferguson and Davis 1972). Currently, it is extensively documented that As is adsorbed onto different mineral surfaces (Bowell 1994a; Diamadopoulos and others 1993; Fuller and others 1993; VarderHock and others 1994; Goldberg and Glaubing 1988). Iron oxyhydroxides are well known for being very good adsorbing substrates for As. Adsorption is a major natural control on the distribution of As, and it is especially important in mining areas where As and other pollutants are being released to the environment (Sweener and others 1994; Wuolo 1986; Qvarfort 1992). Adsorption of As onto iron oxyhydroxide surfaces depends on pH and oxidation state. It has been shown that arsenate [As(V)] is more strongly adsorbed than arsenite [As(III); Gules and others 1979].
The San Antonio-El Triunfo (SA-ET) mining area in southern Baja California peninsula, Mexico, has been exploited for gold and silver since the late 1700s. The mineral extraction processes generated byproducts with high As contents. Chemical analyses of groundwater show high As concentrations (above 0.05 ppm) in the mining area, a though concentrations decrease with increasing distance from the mining area. The SA-ET mining area is located in the recharge area for the San Juan de Los Planes aquifer. This paper explores the possibility of As being adsorbed by the natural aquifer material in the SA-ET area. Experimental data on As adsorption by aquifer material samples from the SA-ET mining area are presented and compared with modeled adsorption of As onto iron oxyhydroxides using the computer codes MICROQL and MINTEQA2 (Allison and others 1991).

Sample description and methods

The samples used for the adsorption experiments were collected directly from the bottom of nine water wells in the SA-ET area using a scoop. The samples were collected and placed in double-sealed plastic bags, then stored in the dark at 4 °C for 2 weeks. In the laboratory, the sam-

ples were analyzed by scanning electron microscopy/EDS and X-ray diffraction in order to determine the mineralogy and minor element content. To determine element content , the samples were digested at 100 °C with HCl and HNO₃ and analyzed by ICP. Untreated sample material was air-dried and sieved to the 100 mesh (0.15 mm) for the adsorption experiments. Three size fractions were used for the adsorption experiments: the 0.15–0.25 mm (coarse) fraction, the <0.15 mm (fine) fraction, and whole-material mix of coarse and fine fractions. The fine material represents ~35% of the whole sample. The coarse material is composed mostly of quartz, feldspar, and fragments of igneous rock (granodiorite-tonalite). The fine material is composed of quartz, feldspar, calcite, illite, chlorite, and hematite/magnetite. The chemical analysis of the fine material shows that it contains ~12 wt% Fe_2O_3. Iron oxide content was not analytically determined in the coarse fraction, but a visual estimate is that it contains <10 wt% Fe_2O_3. Energy dispersive spectra (EDS) from the nine samples showed that there are trace amounts of S, Zn, Cu and As present.

Adsorption experiments

These experiments were carried out using plastic containers as batch reactors with 50 ml double-deionized MILLI-Q water. Background solutions with ionic strengths of 0.1 and 0.01 M $NaNO_3$ were used for different experiments. Only one experiment (the first) used 0.1 M $NaHCO_3$ as a background electrolyte. Different amounts of material were used to obtain total solid-phase iron concentrations between 0.01 and 0.001 M. Total As concentrations used ranged between 3×10^{-5} and 7×10^{-5} M. Arsenic solutions were prepared with As_2O_3 stock standard solution. This solution probably contains both arsenite (H_3AsO_3) and arsenate (H_3AsO_4) and was used for total As analysis (arsenic speciation was not determined). HCl or NaOH was added to solutions to adjust the pH. The experimental solutions were equilibrated for 24 h in the batch reactor and continuously shaken to maintain a constant solid/liquid ratio. After the equilibration, the final pH was measured and the suspension was centrifuged for 10 min at 10000 rpm; 10 ml of the supernatant was filtered through a 0.45 μm membrane, transferred to a vial, and stored in the dark at 4 °C overnight for total As analysis by ICP.

Desorption

To induce desorption, NaOH was added to the samples until the pH reached 12.5. The samples were shaken for 24 h, centrifuged, filtered, and analyzed for total As.

Surface titration

Four surface titration experiments were performed on the natural aquifer material to compare the resulting point of zero charge (PZC) with that of the iron oxyhydroxides (Parks and deBruyn 1962). The setup for the surface titration was the following: a 200 ml plastic bottle with 20 ml double-deionized water and a magnetic stirrer was used as a batch reactor. Nitrogen gas was bubbled through tygon tubing to the solution to exclude CO_2 from the system. A background electrolyte of $NaNO_3$ at different ionic strengths was used. About 0.04 g of aquifer material was used, which corresponds to a Fe solid phase concentration of $\sim 2 \times 10^{-2}$ M. NaOH (0.00125 M) and HCl (0.01 M) solutions were added to raise or lower the pH at constant time intervals (5 min); pH readings were made after the 5-min equilibration time.

Results and discussion

Experimental adsorption

Figure 1 shows the results of the three adsorption experiments; Fig. 1a shows the percent adsorbed vs. pH by the fine and coarse fractions of the aquifer material. The topology of the curves is appropriate for anion adsorption (higher adsorption at low pH and lower adsorption at high pH). The highest adsorption was obtained with the fine-size material. As already mentioned, this material has the highest Fe_2O_3 content (~12%), compared with <10 wt% Fe_2O_3 in the coarse material. The high adsorption (~40%) even at pH 10 is probably due to the highest solid: solution ratio used (total Fe = 0.01 M. This experiment was in $NaHCO_3$ 0.1 M background electrolyte The rest of the experiments used a mix of fine- and coarse-grained material better to represent the natural material. A more typical topology for total As adsorption curves was observed in the second experiment (Fig. 1b). This second experiment used the same amount of solid total Fe phase (0.01 M) as the first set of experiments, but $NaNO_3$ was used as a background electrolyte instead of $NaHCO_3$.

Fig. 1c shows the same experiment as in Fig. 1b, but a lower ionic strength was used ($I=0.01$). The two experiments in Fig. 1b, c look very similar, even though they were conducted in solutions with different ionic strengths. In both cases, the highest percent of adsorption obtained was about 50%. This is probably due to the presence of arsenite (H_3AsO_3) besides arsenate (H_3AsO_4) in the solution. It has been shown that arsenite is less adsorbed onto iron oxyhydroxide surfaces than arsenate under similar conditions (Dzombak and Morel 1990).

The adsorption curve for the third experiment (Fig. 1d) has the right topology, but the maximum adsorption was again fairly low (<40%), suggesting once more the presence of arsenite in the solution. For all the experiments adsorption decreased at high pH (10 to 12), and the maximum adsorption was pH 7–9. Even though these experiments have relatively few points, the results show the expected topology for total As (arsenate + arsenite) adsorption curves and show consistency in the maximum and minimum adsorption ends. When desorption was induced by raising the pH to 12.5, all the samples released all the input As, in some cases, more As than the original amount added was released.

Another experiment was set up to obtain an adsorption isotherm for the aquifer material. Concentrations of As
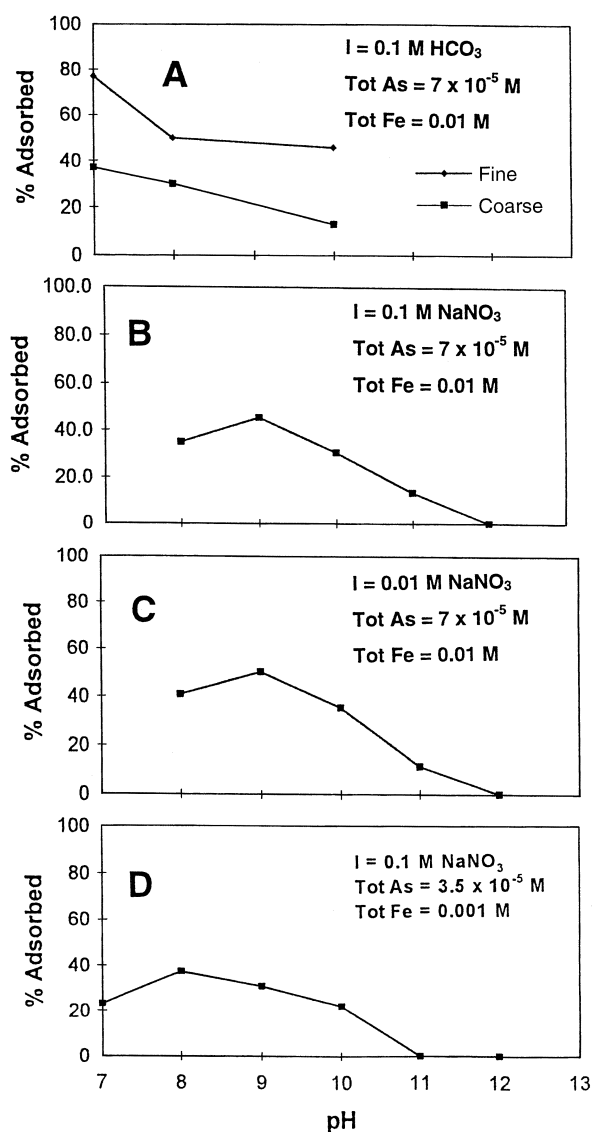
Fig. 1a–d
Percent arsenic adsorbed (experimental results). **a** First experiment using different size fractions (coarse and fine), **b** and **c** second experiment using whole aquifer material but different background electrolyte concentrations, and **d** third experiment

used were 7×10^{-8}, 7×10^{-7}, 7×10^{-6}, 7×10^{-5}, and 7×10^{-4} M; total solid phase Fe concentration used was ~0.02 M. The pH was adjusted to 7. A final experiment was the surface titration of the natural aquifer material. A blank titration was used to correct suspension titrations for supernatant effects (Machesky and Anderson 1986).
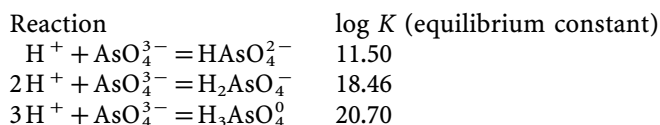
Modeled adsorption

The MICROQL and MINTEQA2 computer codes were used to model adsorption of arsenate and arsenite onto iron oxyhydroxides surfaces. Arsenate and arsenite concentration used in the models equals the concentration of
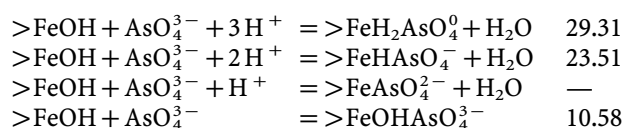
total As used in the experiments ($[As(V)] + [As(III)] = [total As] \sim 7 \times 10^{-5}$ M); the total concentration of solid phase used in the models was a total Fe = 0.01 M. The MICROQL program uses as input data a matrix defining the components in solution (absorbed) and the solid in the solution (adsorbent). The adsorbent used was >FeOH with the following speciation reactions (surface speciation):
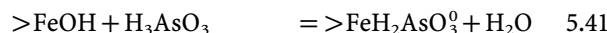
Reaction	log K (equilibrium constant)
$>FeOH + H^+ = >FeOH_2^+$	8.93
$>FeOH = >FeO^- + H^+$	7.29
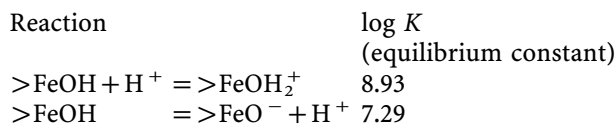
The reaction for the speciation reaction of the arsenate (H_3AsO_4) are:

Reaction	log K (equilibrium constant)
$H^+ + AsO_4^{3-} = HAsO_4^{2-}$	11.50
$2H^+ + AsO_4^{3-} = H_2AsO_4^-$	18.46
$3H^+ + AsO_4^{3-} = H_3AsO_4^0$	20.70

The reactions for the surface speciation between >FeOH and AsO_4^{3-} are:

$>FeOH + AsO_4^{3-} + 3H^+ = >FeH_2AsO_4^0 + H_2O$	29.31
$>FeOH + AsO_4^{3-} + 2H^+ = >FeHAsO_4^- + H_2O$	23.51
$>FeOH + AsO_4^{3-} + H^+ = >FeAsO_4^{2-} + H_2O$	—
$>FeOH + AsO_4^{3-} = >FeOHAsO_4^{3-}$	10.58

The surface complexation reaction for >FeOH and arsenite (H_3AsO_3) is:

$>FeOH + H_3AsO_3 = >FeH_2AsO_3^0 + H_2O$	5.41

The database used for the equilibrium constant values and other adsorption parameters was from Dzombak and Morel (1990). The input matrix for MICROQL contains the stoichiometric coefficients of the reactions, the values of log K and the adsorbate parameters (specific surface area, surface-site density, capacitance of the inner layer). Table 1 shows the input matrix for arsenate adsorption. Table 2 shows the input data for the modeling of arsenite adsorption. To test the model, the first run was set to reproduce the arsenate speciation diagram. Figure 2 shows the results of this modeled speciation, which reproduce the different pK's values (2.24, 6.96 and 11.50). Figure 3 shows the results for modeled arsenate, arsenite and total As adsorption (assuming arsenate>arsenite; 60% to 40%, respectively) at different ionic strengths ($I = 0.1$ and 0.01 M). The topology of the curves matches the experimental data. As is expected, the calculated curves for arsenate (both in a and b of Fig. 3) show a higher percent adsorbed than those for arsenite adsorption. The concentrations of arsenate used was 4.6×10^{-5} M, the concentration of arsenite used was 3×10^{-5} M; [arsenate] + [arsenite] equals the amount used in the experiments (total As = 7.6×10^{-5} M). The central curve in both Fig. 3a, b represents the total As adsorption (sum of the arsenite + arsenate adsorption curves). The assumption made here was that there is more arsenate than arsenite in the natural system because it is an oxidizing environment (Robertson 1989). Models in Fig. 3a, b are for the same con-

Table 1
Input data for the MICROQL computer code for modeling arsenate (H_3AsO_4) adsorption. Data from Dzombak and Morel (1990). (Constant capacitance model, 10 m^2/g: specific surface area, 0.00007 M: surfaces sites, 1.5 g/l: concentration of adsorbent, 0.1 M: ionic strength, 2.9 F/m^2: capacitance of inner layer.)

	AsO_4 total	>FeOH adsorbent	Surf. Charge charge 1	H^+ free	log K
AsO_4	1	0	0	0	0
$H\,AsO_4^{2-}$	1	0	0	1	11.5
$H_2\,AsO_4^-$	1	0	0	2	18.46
$H_3\,AsO_4$	1	0	0	3	20.7
$>FeOH^{2+}$	0	1	1	1	−8.93
>FeOH	0	1	0	0	0
$>FeOH^-$	0	1	−1	−1	−7.29
$>FeH_2AsO_4$	1	1	0	3	29.31
$>FeHAsO_4^-$	1	1	−1	2	23.51
$>FeAsO_4^{2-}$	1	1	−2	1	−
$>FeOHAsO_4^{3-}$	1	1	−3	0	10.58
H^+	0	0	0	1	0
	0.0003	0.1	0	1E-07	

Table 2
Input data for the MICROQL computer code for modeling arsenite (H_3AsO_3) adsorption. Data from Dzombak and Morel (1990) (details of constant capacitance model in Table 1)

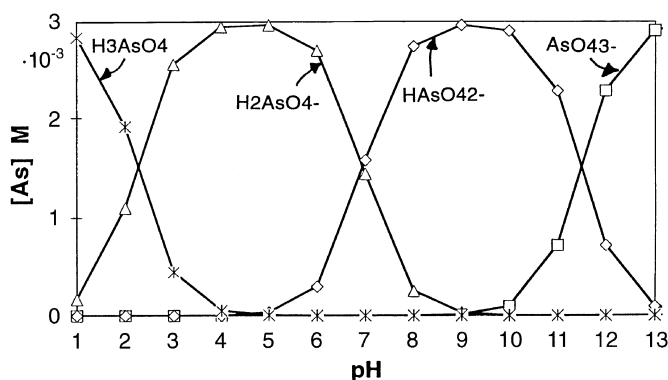|	H_3AsO_3 total	>FeOH adsorbent	Surf. Charge charge 1	H^+ free	log K
H_3AsO_3	1	0	0	0	0
$>FeOH^{2+}$	0	1	1	1	−8.93
>FeOH	0	1	0	0	0
$>FeOH^-$	0	1	−1	−1	−7.29
$>FeH_2AsO_3$	1	1	0	0	5.4
H^+	0	0	0	1	0
	0.0003	0.1	0	1E-07	

Fig. 2
Modeling of arsenate (H_3AsO_4) speciation and reproduction of pK values using the MICROQL computer code (see text for pK values)

ditions, varying only the ionic strength (from $I=0.01$ to 0.001 M).
The MINTEQA2 program allows modeling adsorption of arsenate and arsenite simultaneously. The modeling was done with the same input data as the modeling with MICROQL. Figure 4 shows the results of this adsorption model at different ionic strengths ($I=0.1$ and 0.01 M). Fig. 4a matches the models of MICROQL (Fig. 3a) . The central curve (total As) is the sum of the arsenate and arsenite curves. Fig. 4b slightly differs from the model of MICROQL (Fig. 3b) especially for the arsenite adsorption curve, which shows a convex topology. The total As adsorption curve (Fig. 4b) matches the experimental curves in Fig. 1b, c, d. The convex topology suggests the presence of arsenite in the experimental solutions.
Figure 5 shows the experimental and modeled adsorption isotherms at pH 7. The modeled isotherm (MICROQL) was obtained combining the arsenate and arsenite isotherms, assuming arsenate>arsenite. (60% over 40%, respectively). This modeled total As adsorption isotherm shows a very close match to the experimental isotherm. At high concentration, both curves flatten due to saturation of the available surface sites.
Another very interesting result is the surface titration curve (Fig. 6). The four curves for different ionic strengths cross to give a PZC of between pH 8 and 8.5, which is very close to the PZC for iron-hydroxides (ferri-
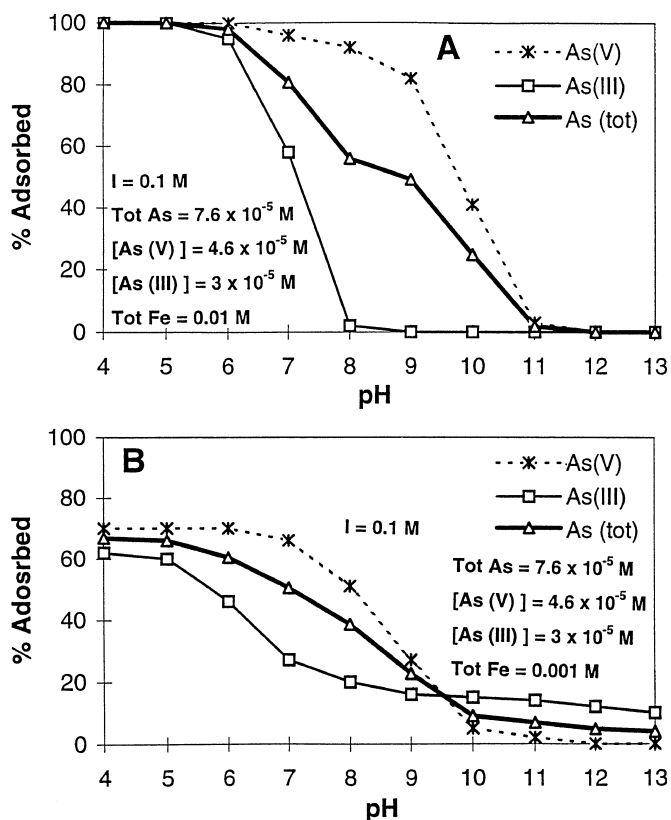
Fig. 3a, b
Modeled percent arsenic (arsenate and arsenite) adsorbed onto iron oxyhydroxides surfaces using the MICROQL code.
a Arsenate and arsenite adsorption under similar conditions, but different concentrations of arsenate and arsenite. b Similar to a, but lower concentration of total Fe in the system. Note that arsenite in both cases (a and b) is less adsorbed than arsenate. The central curve is the sum of arsenate and arsenite adsorption

Fig. 4a, b
Modeled percent arsenic (arsenate and arsenite) adsorbed onto iron oxyhydroxides surfaces using the MINTEQA2 code.
a Simultaneous adsorption of arsenate and arsenite. The central curve is the sum of arsenate and arsenite adsorption curves and represents the total arsenic adsorbed. b Similar to a, but lower concentration of total Fe in the system. Note that arsenite in both cases (a and b) is less adsorbed than arsenate. The central curve is the sum of arsenate and arsenite adsorption

Fig. 5
Total As adsorption isotherm at pH 7 and 25 °C. Modeled isotherm using the MICROQL code. From the experimental data a distribution coefficient K_d of about 1.86 was estimated

hydrite = 7.9–8.2; Parks and deBruyn 1962; Dzombak and Morel 1990).

Thus, despite the mineralogical complexity of the natural aquifer material in the SA-ET mining area, the experimental adsorption results show that it is plausible that the surfaces of iron oxyhydroxides in the material are the principal adsorbate in the system. Although other mineral surfaces in the natural aquifer material are very lekely interacting with the As (Jacobs and others 1970; Goldberg and Glaubig 1988), the experimental data show that it is plausible that iron oxyhydroxides are the main material adsorbing As in the natural environment in the filed area. This is a natural control of the As leaching into the groundwater from the mine-waste material in the SA-ET mining area.

Based on the experimental data (Fig. 5), a distribution coefficient for the aquifer material (Kd = [total As]surf/ [total As] sol) of about 1.86 was calculated. An estimate of the retardation factor (R) (Stumm and Morgan 1996; Drever 1988) and of the travel time for the As plume from the SA-ET area towards Los Planes aquifers is
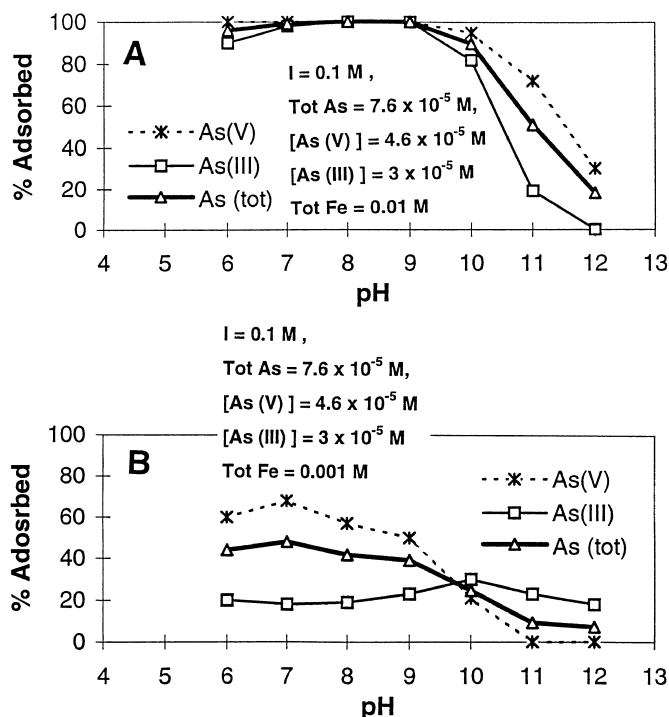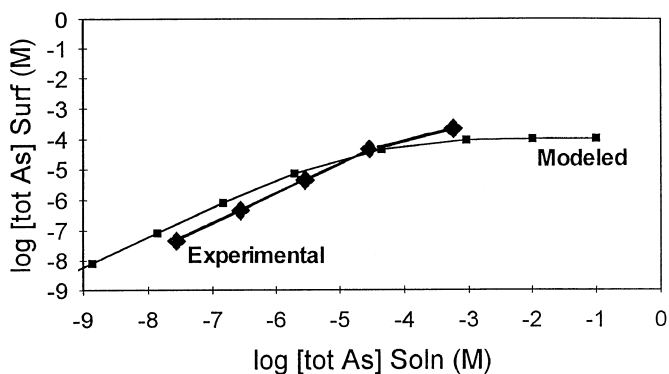
shown in Table 3. The lowest and highest values for the hydraulic conductivity (K) and porosity (n) used for this calculation are extreme values for fractured igneous rock and alluvial material (Freeze and Cherry 1979). The change in density with changing porosity was not included in the calculation. Based in this crude calculation,

Table 3
Estimated travel time for the arsenic plume from the SA-ET mining area towards the Los Planes aquifer. K = hydraulic conductivity; dh/ds = hydraulic head gradient; R = retardation factor; $Dens$ = bulk density of the aquifer material (g/cm^3); n = porosity

SA-ET area $dh/ds = 0.02$		$Dens = 2.5$		Valley $dh/ds = 0.01$		$Dens = 2$		
K (m/s)	n (%)	R	time (years)	K (m/s)	n (%)	R	time (years)	Total time (years)
1E-08	2	234	6 318 282	1E-06	15	26	501 094	6 819 376
1E-06	4	117	63 453	1E-04	25	16	5 140	68 594
1E-04	10	48	643	1E-02	40	10	53	696
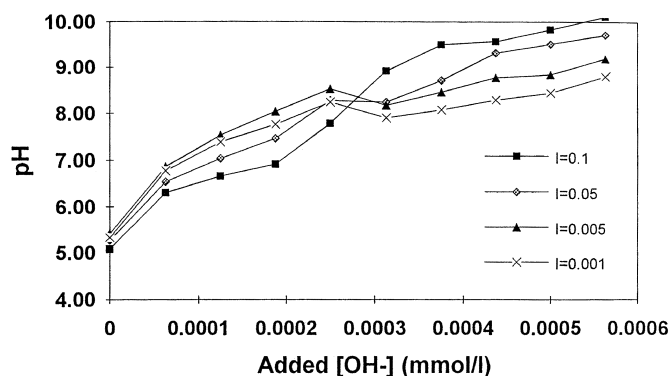
Fig. 6
Surface titration curves used to determine the point of zero charge (PZC) of the aquifer material. Background electrolyte used was NaNO$_3$. See text for details

an estimate for R ranges between 50 and 70. An estimate for the As plume travel time from the SA-ET mining area towards Los Planes area is between 700 and 5000 years. Thus the natural aquifer material is acting as a good natural control for the As contamination.

Conclusions

Fe$_2$O$_3$ content in the fine fraction of the aquifer material is ~ 12 wt% . In the coarse fraction the Fe$_2$O$_3$ content is < 10 wt%.
Experimental adsorption curves show the expected topology for total As adsorption ([arsenate] + [arsenite]; high adsorption at low pH and low adsorption at high pH).
The presence of arsenite in the experimental solutions is suggested by the < 100% adsorbance.
The experimental total As adsorption isotherm at pH = 7 indicates saturation of adsorbing sites at high concentrations; surface titration of the aquifer material indicates a PZC ~ 8–8.5 (iron oxyhydroxides = 7.9–8.2).
Comparison between modeled and experimental total As adsorption suggests that As is being adsorbed mostly by iron oxyhydroxides surfaces in the natural environment.

A distribution coefficient for the aquifer material $Kd = 1.07$ was calculated based on the experimental data. Estimates of the retardation factor (R) suggest that the As plume travel time from SA-ET area to Los Planes area is about 700 to 5000 years.

References

ALLISON JD, BROWN DS, NOVOGRADAC KJ (1991) MINTEQA2/ PRODEFA2, a geochemical assessment model for environmental systems: version 3.0 User's Manual. EPA/600/3-91/021, Washington, DC: US

BOWELL RJ (1994a) Sulfide oxidation and arsenic speciation in tropical soils. Environ Geochem Health 16 (2):84–91

BOWELL R J (1994b) Sorption of arsenic by iron oxides and oxyhydroxides in soils. Appl Geochem 9:279–286

DIAMADOPOULOS E, IOANNIDIS S, SAKELLAROPOULOS G (1993) As(V) removal from aqueous solutions by fly ash. Water Res 27:1773–1777

DREVER JI (1988) The geochemistry of natural waters. Prentice Hall, New Jersey

DZOMBAK DA, MOREL FM (1990) Surface complexation modeling (hydrous ferric oxide). Wiley, New York

ENTERLINE PE, HENDERSON VL, MARSH GH (1987) Exposure to arsenic and respiratory cancer (a reanalysis). Am J Epidemiol 125:929–935

FERGUSON JF, DAVIS J (1972) A review of the arsenic cycle in natural waters. Water Res 6:1259–1274

FOWLE III JR (1992) Health effects of arsenic in drinking water: research needs. Environ Geochem Health 14 (2): 63–68

FREEZE RA, CHERRY JA (1979) Groundwater. Prentice Hall, New Jersey

FULLER C, DAVIS J, WAYCHUNAS G (1993) Surface chemistry of ferrihydrite: part 2. Kinetics of arsenate adsorption and coprecipitation. Geochim Cosmochim Acta 57:2271–2282

GOLDBERG S, GLAUBING (1988) Anion sorption on a calcareous montmorillonitic soil-arsenic. Soil Sci Soc Am J 52:1297–1300

GOLDMAN M, DACRE JC (1991) Inorganic arsenic compounds: are they carcinogenic, mutagenic, teratogenic? Environ Geochem Health 13 (4):179–191

GULES J, CHAMP D, JACKSON R (1979) Influence of redox environments on the mobility of arsenic in groundwater. In: Jenne E (ed.) Chemical modeling in aqueous systems. ACS Symposium Series 93:81–95. Washington, DC: American Chemical Society

JACOBS LM, SYERS JK, KEENEY DR. (1970) Arsenic sorption by soils. Soil Sci Soc Am J 34:750–754

Machesky LM, Anderson MA (1986) Calorimetric acid base titrations of aqueous goethite and rutile suspensions. Am Chem Soc Langmuir 2:582–587

Parks GA, deBruyn PL (1962) The zero point of charge of oxides. J Phys Chem 66:967–973

Qvarfort V (1992) The high occurrence of arsenic in Macadam products from an iron mine in central Sweden: significance for environmental contamination. Environ Geochem Health 14(3):87–90

Robertson FN (1989) Arsenic in groundwater under oxidizing conditions, southwest USA. Environ Geochem Health 11(3–4):171–185

Stumm W, Morgan JJ (1996) Aquatic chemistry: chemical equilibria and rates in natural waters. 3rd edn. Wiley, New York

Sweener R, Vankeer I, DeVos W (1994) Heavy metal contamination in overbank sediments of the Geul River (east Belgium): its implications to former Pb-Zn mining activities. Environ Geol 24:12–21

VanderHock E, Bonouvrie T, Comans J (1994) Sorption of As and Se on mineral components of fly ash: Relevance for leaching processes. Appl Geochem 9:403–412

Wuolo RW (1986) Laboratory studies of arsenic adsorption in alluvium contaminated with gold-mine tailings along Whitewood Creek, Blackhills, South Dakota. MSc Thesis. South Dakota School of Mines